Please Return to me.

EXPERIMENT 3

GAMMA RAY DETECTION WITH SCINTILLATION DETECTORS

PURPOSE

1. To demonstrate the use of a sodium iodide scintillation detector and its response to gamma rays.
2. To show the absorption of gamma rays in matter.

EQUIPMENT REQUIRED

Model 802–3 NaI(Tl) Scintillation Detector
Model 802–5 Tube Base
Model 805 Preamplifier
Model 2012 Amplifier
Model 2000 Bin and Power Supply
Model 3102 High Voltage Supply
OMEGA–1 Multichannel Analyzer
Oscilloscope
Model A501 Absorber Set
Model 7443 Gamma Reference Source Set
Model 7445 Coincidence Source Set
Model C177–3 Coaxial Cable Set

ADDITIONAL EQUIPMENT FOR PART D

Model 1772 Counter/Timer

A. RADIOACTIVE SOURCES AND SCINTILLATION DETECTORS

Radioactive nuclei decay by emitting beta or alpha particles. Often the decay is to an excited state of the daughter nucleus, which usually decays by emission of a gamma ray. The energy level sequence and therefore the gamma ray energy spectrum for every nucleus is unique and can be used to identify the nucleus. The energy levels and decay processes of ^{22}Na, ^{60}Co, and ^{137}Cs are given in Figure 3.1. The term beta decay means either $\beta-$ (electron) emission, $\beta+$ (positron) emission, or electron capture by the nucleus.

The thallium-activated sodium iodide detector, or NaI(Tl) detector, responds to the gamma ray by producing a small flash of light, a scintillation. The scintillation occurs when electrons, and in some cases positrons, are given energy by the incident gamma ray and are stopped by the crystal. The crystal is mounted on a photomultiplier tube that converts the scintillation to an electrical pulse. The first pulse from the photocathode is very small and is amplified in 10 stages in a series of dynodes to get a large enough pulse. This is taken from the anode of the photomultiplier, and is a negative pulse.

The NaI crystal is protected from collecting moisture in the air by encasing it in aluminum, which also serves as a convenient mounting for the entire crystal photomultiplier unit.

There are three dominant gamma ray interactions with matter:

1. The photoelectric effect
2. The Compton effect
3. Pair production

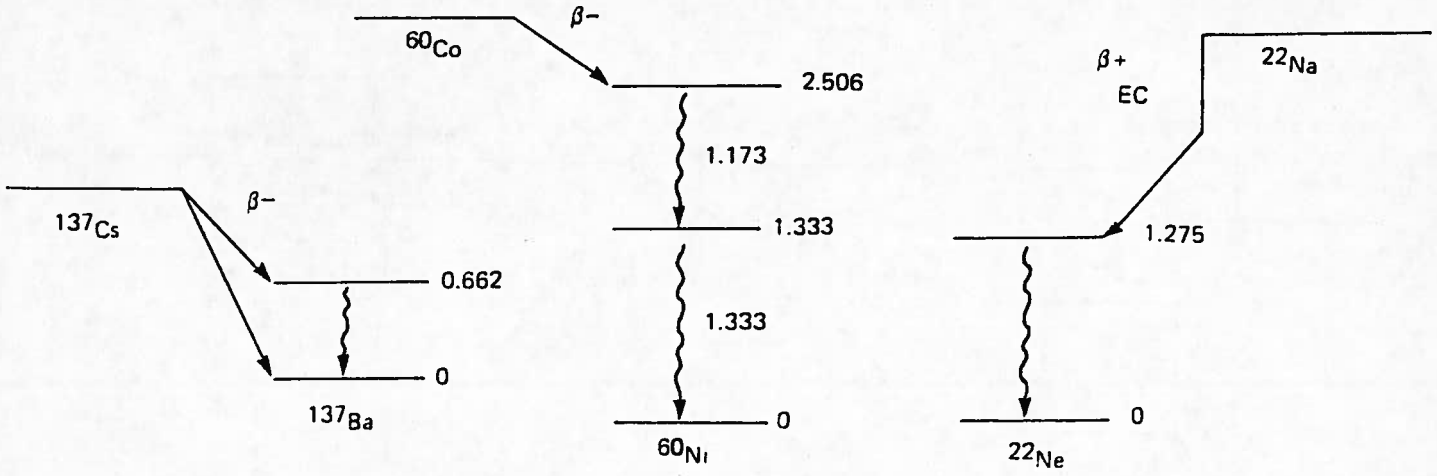

Figure 3.1 Decay Schemes.

Only the photoelectric effect produces an output pulse that is proportional to the gamma ray energy. In the photoelectric effect, all of the energy of the gamma ray is absorbed by an electron. In the Compton effect, the gamma ray scatters from an electron, giving the electron an amount of energy that depends upon the angle of scatter:

$$E' = \frac{E}{1 + \frac{E}{mc^2}(1 - \cos\theta)}$$

where E' is the scattered gamma ray energy, E the incident gamma ray energy, and θ is the angle of scatter. The term mc^2 is the rest mass energy of the electron, equal to 0.511 MeV. The energy given the electron is just

$$E_e = E - E'$$

If the gamma ray escapes from the crystal, then the only energy deposited is the electron energy, and the output pulse is much less than that for the full energy. The spectrum is complicated by having many pulses not of the full gamma ray energy, as will be seen below.

If the gamma ray does not escape from the crystal, but either scatters again or gives up its remaining energy by the photoelectric process, then the full energy pulse is obtained. Since this is more likely in a larger crystal, the full energy efficiency increases by more than the increase in volume.

Pair production occurs when the gamma ray energy is greater than 1.022 MeV, but is not an important part of detection until energies of 2.5 MeV or higher. The positron and electron of the pair produced slow down and scintillate, just as for Compton scattered electrons. When the positron comes to rest it annihilates with an electron, producing two 0.511 MeV gamma rays. Both of these must be absorbed to get the full energy peaks. Pair production will be discussed further in Experiment 4.

The maximum energy given to an electron in Compton scattering occurs for gamma ray scattering of 180°, and the energy distribution is continuous up to that point. This energy, known as the Compton edge, can be calculated from the incident gamma ray energy.

B. GAMMA RAY SPECTRUM

1. Connect the apparatus as in Figure 3.2. Place the ^{137}Cs source near the NaI detector and set the HV supply at +1000 volts. Set the amplifier gain and polarity so that the peak appears a little below the middle of the display. Collect the data long enough so that the spectrum appears to vary smoothly from one point to the next. It should appear as in Figure 3.3A. Identify the photopeak. The mass of data to the left of the photopeak is the Compton distribution, which has a maximum value at the Compton Edge. This is the response to a monoenergetic gamma ray of roughly medium energy. A very strong peak at low energy may be present if the discriminator is set low enough. This is the Ba x-ray at 37 keV, which follows internal conversion.

2. Read out the spectrum and make a graph of it.

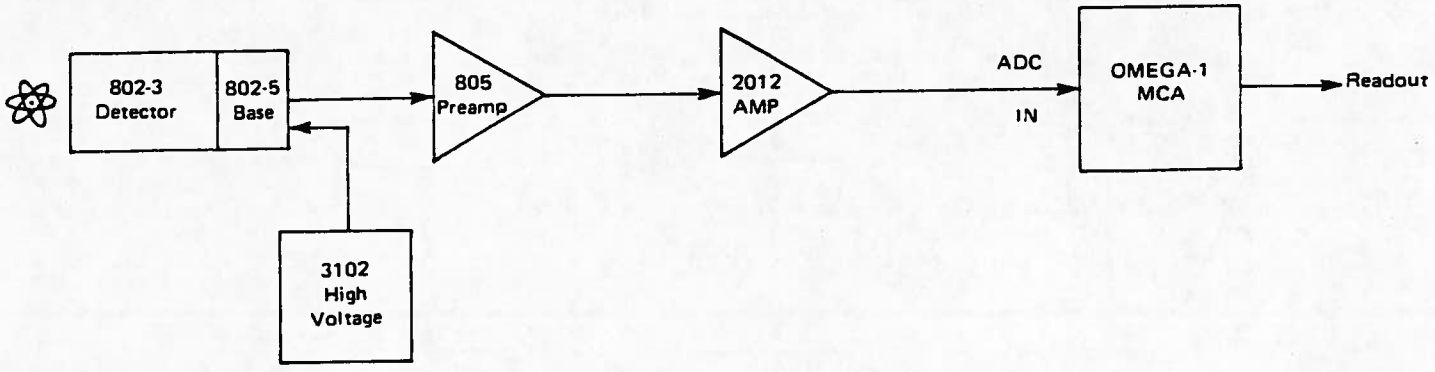

Figure 3.2 Electronics Setup.

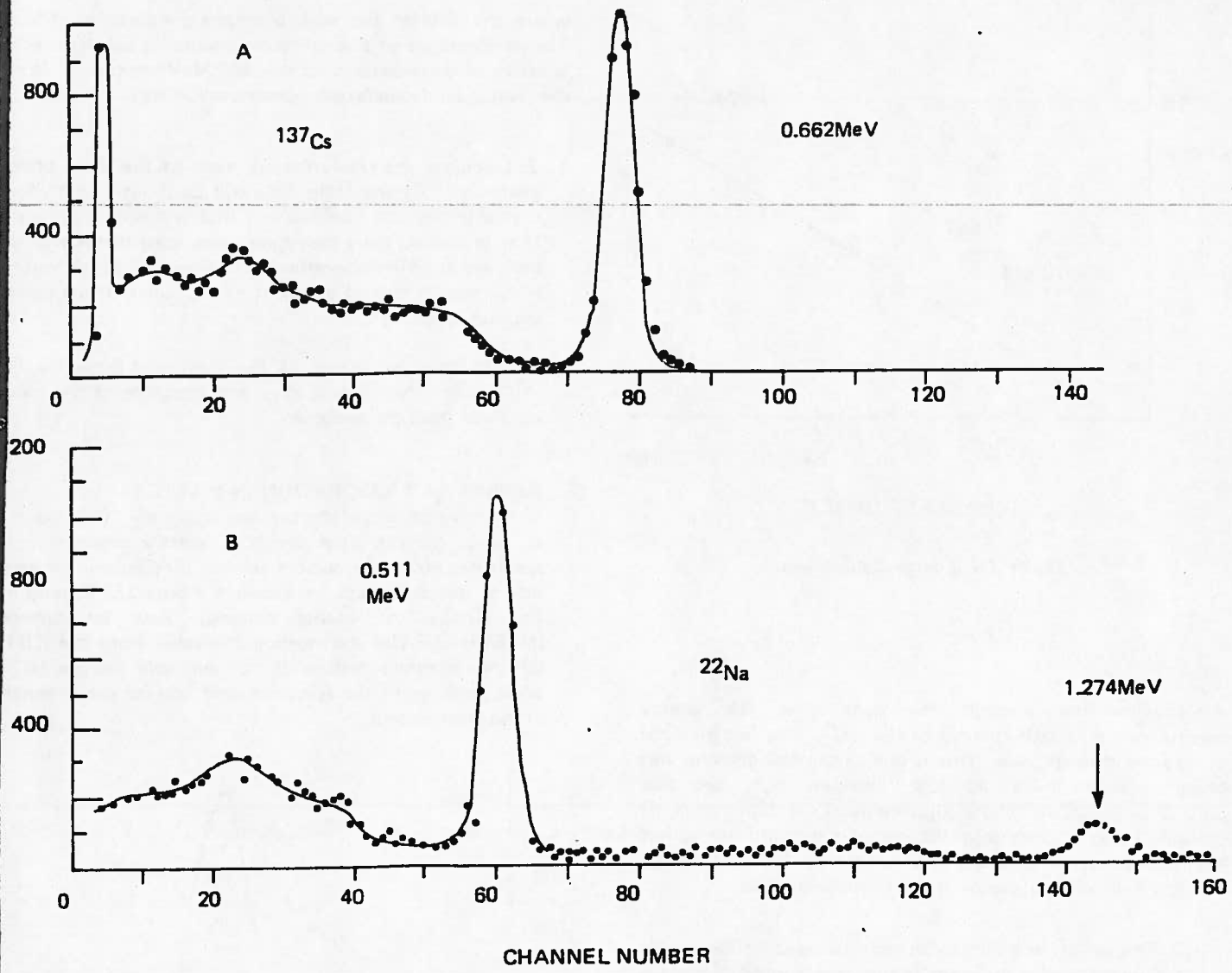

Figure 3.3 Gamma Ray Spectra.

3. Now place the ^{22}Na source near the detector instead of the ^{137}Cs source. Clear the memory and collect a spectrum. From the decay scheme (Figure 3.1) one could expect a similar spectrum to ^{137}Cs, but there are now two peaks. The higher one at 1.27 MeV is the gamma ray expected, while the lower one is at 0.511 MeV and is the radiation from positron annihilation. This "511" radiation will always be present when positrons are emitted by nuclei. Read out the spectrum and plot a graph of it. It should appear as in Figure 3.3B.

4. Place a large piece of lead (such as a lead brick) next to the source and take a fresh spectrum. There will be additional counts in the Compton region of the spectrum due to scattering from the lead. Any material near the source will cause scattering of gamma rays, so this effect cannot be entirely eliminated.

C. ENERGY CALIBRATION AND RESOLUTION

1. From the graphs of the ^{137}Cs and ^{22}Na spectra determine the central channel of each photopeak and plot the gamma ray energy of the peak vs. the corresponding channel. (Alternatively, move the cursors to the peak channel and read the cursor channel from the display.) Estimate the position to the nearest channel, and estimate the uncertainty in determining the peak position. Plot the uncertainty in position as error flags, as in Figure 3.4.

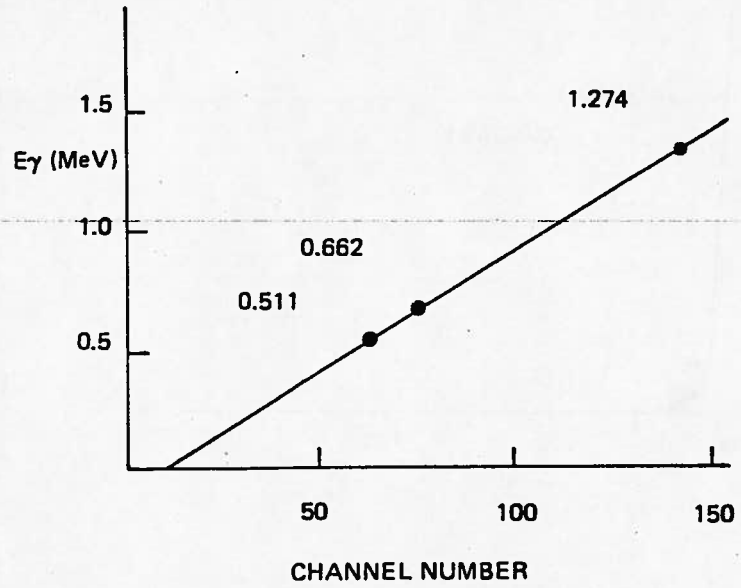

Figure 3.4 Energy Calibration.

A straight line through the data gives the energy corresponding to each channel of the MCA. The line may not go exactly through zero. This is due to the NaI detector not being exactly linear at low energies, but can also be due to variations in the adjustment of the zero setting of the ADC. Non-linearity may also occur if the amplifier gain is high enough to bring pulses into saturation, but this can be checked with an oscilloscope at the amplifier output.

2. The calibration curve can now be used to determine the energies of a different gamma ray source. Collect a spectrum for ^{60}Co and determine the energies of the two photopeaks that appear.

The uncertainty in the peak position is related to the width of the peak. The full width of the peak at half of its maximum value (FWHM) is used to determine the resolution by:

$$\text{RESOLUTION} = \frac{\text{FWHM} \times 100\%}{\text{Peak Position}}$$

where the FWHM and peak positions are given in channels. The performance of a scintillation counter is usually specified in terms of its resolution for the .662 MeV peak of ^{137}Cs since the resolution depends upon gamma ray energy.

3. Calculate the resolution for each of the three photopeaks in ^{137}Cs and ^{22}Na. This will be about 8 to 9% for a crystal-phototube combination that is working properly. If it is higher, there may have been some damage to the unit, resulting in poor optical coupling, or the high voltage is too low (it should be about +1000 volts), or the counting rate is too high.

4. Calculate the energy of the Compton Edge for the ^{137}Cs and ^{22}Na gamma rays and compare to the value obtained from the spectrum.

D. GAMMA RAY ABSORPTION IN MATTER

1. Remove all other sources and place the ^{137}Cs source at about 10 cm from the NaI detector and collect a spectrum. Move the cursors so that they appear on each side of the photopeak, as shown in Figure 3.5. Determine the number of counts between them by turning INTEGRATE ON and reading the value from the CRT. (If the integrate feature is not available on the MCA being used, print the spectrum and add up the channels of the photopeak.)

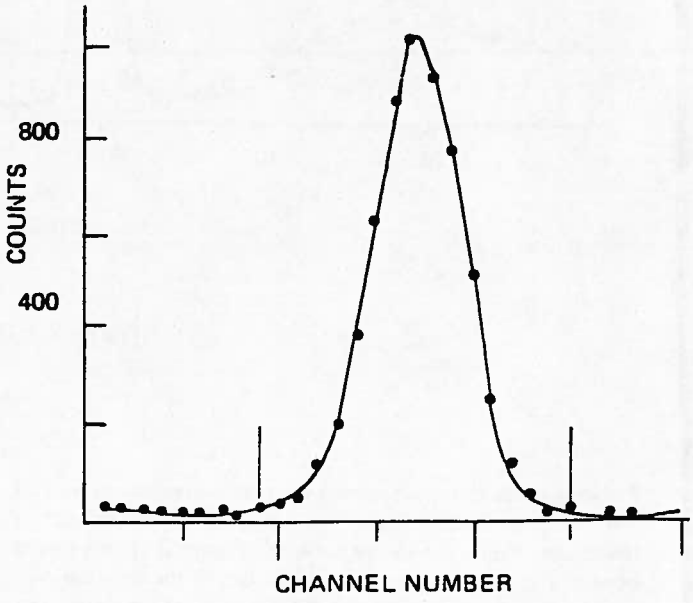

Figure 3.5 Peak Area.

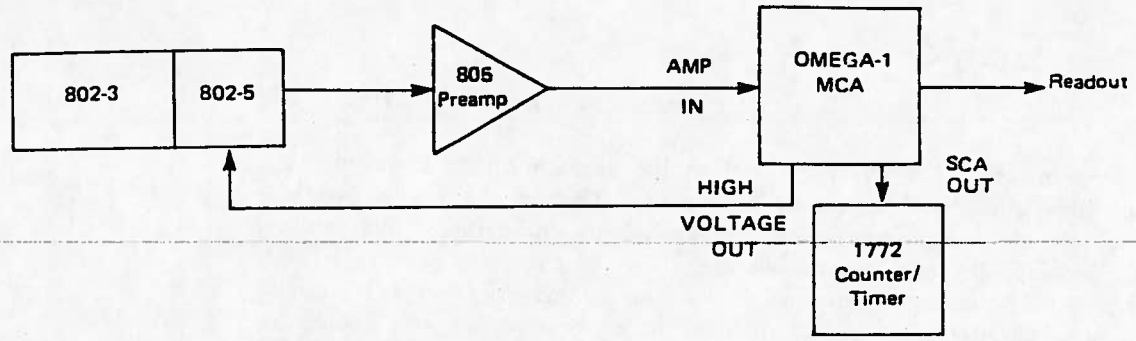

Figure 3.6 Electronics Setup.

Connect the Model 1772 Counter/Timer input to the CA SCA output. The SCA output from the back of the CA is now set to give pulses for just the photopeak. ount these photopeak pulses for 100 seconds.

Place one sheet of lead between source and detector d count the number of pulses in 100 seconds. Repeat th an additional sheet of lead each time.

Remove the ^{137}Cs source and determine the back-ound counts in the photopeak region in 100 seconds. ubtract the background from each of the data taken ove. Calculate the error in the result from:

$$\sigma_{TOTAL} = \sqrt{\sigma^2_{data} + \sigma^2_{background}}$$

Plot the logarithm of the number of counts (and the ror flags) vs. the absorber thickness of lead. Determine e absorption coefficient from the slope of the curve nce:

$$\log\left(\frac{I}{I_0}\right) = -\mu x$$

where I is the intensity for the thickness x and I_0 is the ntensity with no absorber. The absorption coefficient μ s usually expressed in units of cm^{-1}.

ULTICHANNEL ANALYZER DEAD TIME

nultichannel analyzer requires many microseconds longer the input pulse width to convert the pulse to a memory on and increment that location. During that time the is dead and will not accept any more pulses. A meter e front of the MCA gives a measure of the percent of that it is dead. The internal clock used in the preset time is corrected for the dead time, so that the preset time used is live time, and is always longer than clock time. Channel zero is incremented every second of live time in order to have a value of elapsed live time with the spectrum.

1. Use the equipment as set up above, according to Figure 3.2 but with a Model 1772 Counter/Timer connected to the SCA output. Place the ^{137}Cs source such that the dead time meter reads about 10 to 20%. Set the preset time at 100 seconds on the MCA and on the Model 1772 Counter/Timer. Start the Counter/Timer and MCA at the same time, and collect a spectrum and SCA output counts.

2. Record the following values: Elapsed live time (channel zero), preset time, scaler counts (SCA output), and MCA photopeak counts (by integrating the spectrum, or by printing the spectrum and summing the channels).

3. Calculate the ratio of MCA photopeak counts to scaler counts. Expressed as percent, this ratio is the live time of the MCA, and should be about the same as the value 100% ADC dead time. The elapsed live time and preset time should have the same value.

References

1. J.H. Neiler and P.R. Bell, "The Scintillation Method" Alpha, Beta, and Gamma Ray Spectroscopy, K. Siegbahn, ed., North-Holland, Amsterdam, (1965), pp. 245–302.
2. F. Ajzenberg-Selove, ed., Nuclear Spectroscopy, Academic Press, New York, (1960), pp. 211–334.
3. W.J. Price, Nuclear Radiation Detection, McGraw-Hill, New York, (1968).
4. J.B. Birks, The Theory and Practice of Scintillation Counting, MacMillan, New York (1964).

room temperature. However, by cooling the germanium to liquid-nitrogen temperatures, this problem can be alleviated. Methods have also been developed to reduce the conductivity produced by impurities, thus making feasible depletion layers of 1 cm thickness.

Figure 7–19 shows, as an example, part of the gamma-ray spectrum obtained with a germanium counter from a nitrogen target bombarded with deuterons. The left-hand peak results from the decay of the first excited state of N^{15} produced in the $N^{14}(d, p)N^{15}$ reaction. The event in the detector material is pair production of a 5.25-MeV gamma ray depositing 4.23 MeV in the material from the stopping of the electron and the positron. The positron is annihilated in the detector but the annihilation radiation, two 0.51-MeV gamma rays, escapes. Events in which one or both of the annihilation quanta are absorbed give rise to other (smaller) peaks in the pulse-height spectrum, corresponding to deposited energies of 4.74 and 5.25 MeV. The right-hand peak corresponds in similar fashion to the decay of the second excited state of O^{15} produced in the $N^{14}(d, n)O^{15}$ reaction. In many of the events, of course, the electron and/or positron may not come to complete rest inside the material. This gives rise to a reduced voltage pulse, contributing to the more or less continuous background shown in Fig. 7–19.

7–7 *The Scintillation Counter*

The famous measurements by Rutherford and his associates of alpha particles scattered from thin metal foils were performed by viewing the scintillations caused by the alpha particles impinging on a zinc sulfide screen. The photons in the visible range produced by the slowing-down process of the alpha particles were directly viewed by the eye through a low-power microscope. A modern scintillation counter operates on exactly the same principle, except that the human eye is replaced by an electronic device called *a photomultiplier tube*. Figure 7–20 shows schematically the arrangement. Photons produced in the scintillation crystal cemented to the surface of the photomultiplier tube liberate electrons from the photocathode. These electrons are accelerated over approximately 100 to 300 V and are electrostatically focused so that they impinge on the first dynode. By the impact, a number of secondary electrons are released, usually of the order of 2 to 5 per primary electron. The secondary electrons are accelerated again across the gap to the second dynode, where the number is further multiplied. A photomultiplier tube usually contains 10 to 15 dynodes, each with a multiplication factor of 2 to 5, depending on the voltage between the dynodes. Photons striking the photocathode therefore cause an avalanche of electrons which eventually hits the anode and produces a voltage pulse over the resistor R. This voltage pulse is proportional to the energy deposited by the primary radiation in the crystal, or approximately so. The scintillation counter therefore can be used as a spectrometer in conjunction with an electronic pulse-height analyzer.

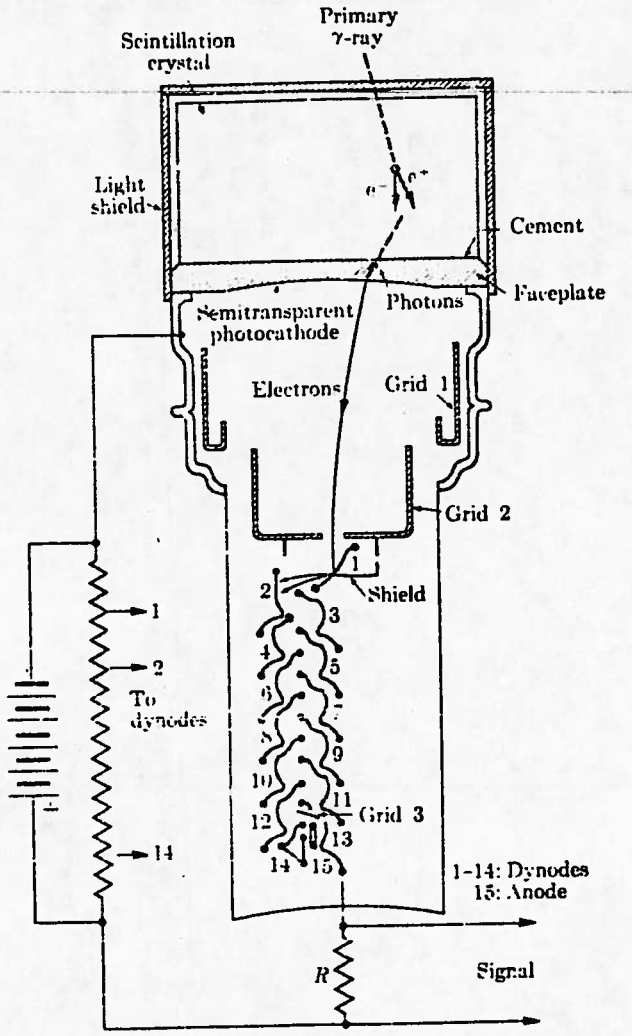

Fig. 7–20. Large scintillation crystal (for gamma rays) and photomultiplier tube (RCA 7046).

Table 7–3 lists the properties of several of the common phosphors used in scintillation counters or spectrometers. Column 5 of the table lists the decay constant; that is, the time it takes for the phosphor to release its stored-up energy in the form of photons. The slowest of the crystals, the cesium iodide crystal, is still much faster than a Geiger-Mueller tube, which has a dead time of about 10^{-4} sec. The importance of fast response in nuclear detectors is discussed in Section 8–6.

Table 7–3. Properties of some common phosphors used as scintillation detectors*

Phosphor	Density, gm/cm^2	Index of refraction	Relative response	Decay constant ($\times 10^{-9}$ sec)	Approximate range of a 10-MeV proton,[a] mg/cm^2	Remarks
Anthracene	1.25	1.59	1.00	30	107	Response standard with RCA 5819 or equivalent phototube
trans stilbene	1.16		0.60	6.4	105	
p-terphenyl in toluene	0.86	1.50[b]	0.35	2.2	99	Typical liquid scintillator at 5 gm/liter concentration of terphenyl
p-terphenyl in polystyrene	1.06	1.59[c]	0.39	4.0	101	Typical plastic scintillator 36 gm/liter of monomer 0.2 gm/liter of 1,1,4,4, tetraphenyl-1,3-butadiene
NaI(Tl)	3.67	1.77	2.10	250	250	
CsI(Tl)	4.51	1.79	0.5	1100	260	
ZnS(Ag)	4.09	2.4	1	10^4	190	
			4[d]			Not available except as powder, partially opaque to own radiation

* From N. S. Wall, *Nuclear Spectroscopy*, ed. Fay Ajzenberg-Selove, Part A. New York: Academic Press, 1960, p. 39. (Reprinted by permission.)

[a] Computed from range-energy curves of Aron *et al.*, AECU 663 revised

[b] For pure solvent

[c] For pure polymer

[d] ZnS has a large light output when the signal is integrated over long times.

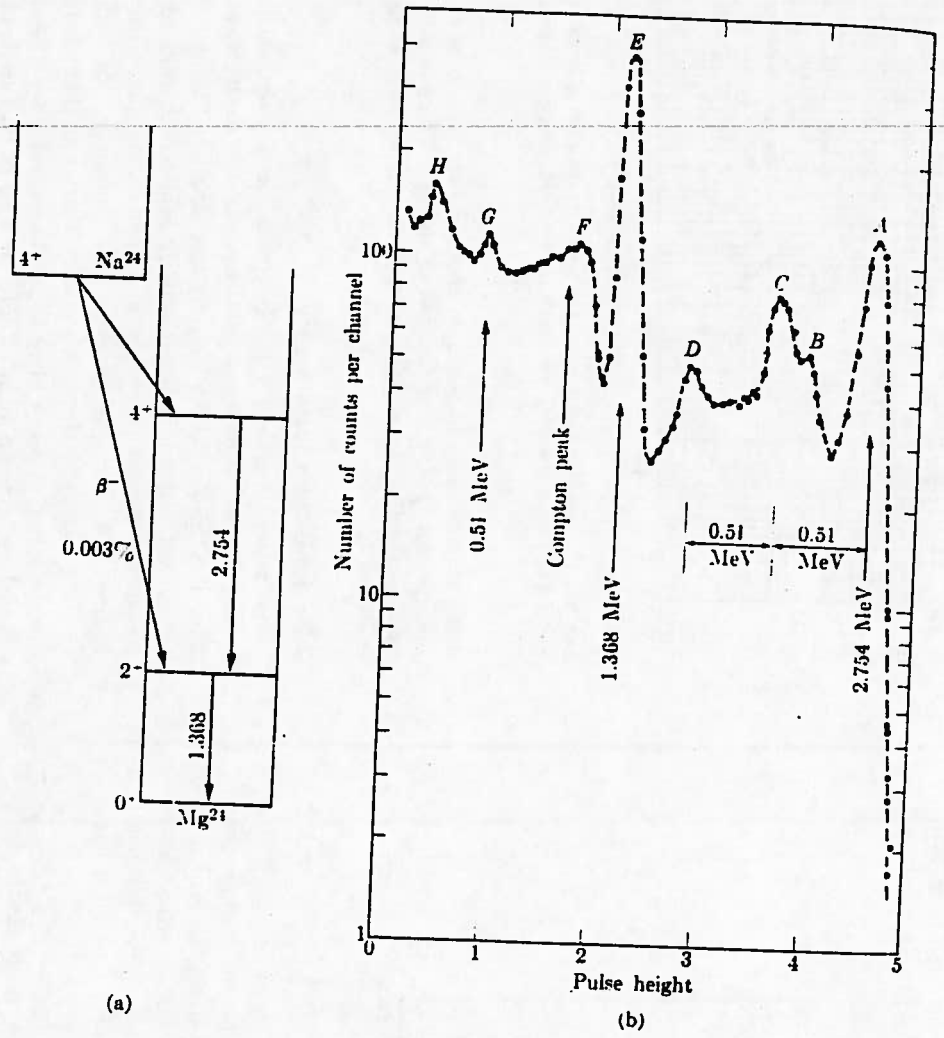

Fig. 7–21. (a) Decay scheme for Na^{24} and (b) pulse-height spectrum for the gamma rays emitted in the decay obtained with a 3-in. × 3-in. NaI scintillation crystal. (Data from P. R. Bell in *Beta- and Gamma-Ray Spectroscopy*, ed. by K. Siegbahn. Amsterdam: North-Holland Publishing Company, 1955.)

The scintillation spectrometer has found many applications in low-energy, as well as in high-energy, nuclear physics. It has been particularly popular in the area of gamma-ray spectroscopy, for which usually a large (e.g., 3-in. diameter, 3-in. thick) NaI crystal is used. Unfortunately, even monoenergetic gamma rays produce a complex pulse-height spectrum, reflecting the fact that varying amounts of the gamma-ray energy may be deposited in the crystal.

particles are monoenergetic; (2) the changes in direction of the electrons in collisions may easily be great, where for alpha particles they are small; and (3) the straggling is much greater for electrons than for alpha particles because in electron-electron collisions, a large fraction of the incident energy can be transferred in a single encounter. The shape of the curve of Fig. 7 will vary with the

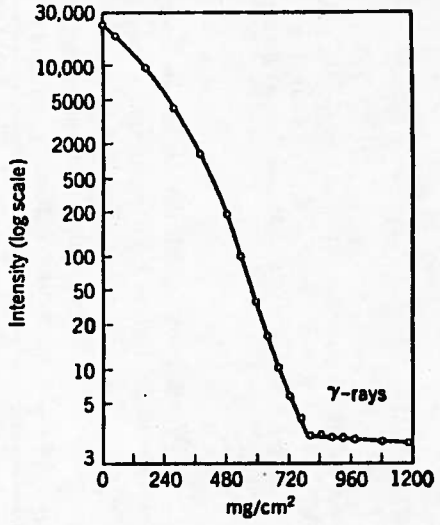

FIG. 7. A semilogarithmic absorption plot for beta rays from P^{32}. The detector was an ionization chamber. From Wu (W41).

geometrical arrangement. Only the end point will remain unchanged. If there are nuclear gamma rays, a background due to them will be superimposed upon the electron curve. Absorption curves for monoenergetic conversion electron emitters, although of somewhat different shape than the curve of Fig. 7, also have characteristic end points.

One can construct an end point versus maximum energy plot for beta emitters, in analogy with Fig. 5. End points cannot be determined reproducibly with any accuracy by inspection, however; nor can one use simple extrapolation because the curve of Fig. 7 is not linear. An extrapolation technique that can be used relies on a comparison of the absorption curve of the unknown beta emitter with one of a standard beta emitter of known end point, in the same geometry. This method, first developed by Feather (F38) has been extended by Bleuler and Zunti (B146). Figure 8

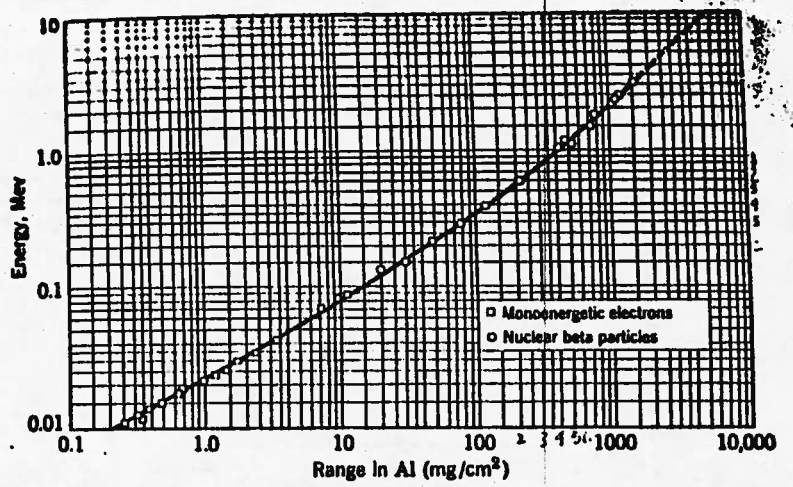

FIG. 8. End points in aluminum for nuclear beta rays of various maximum energies and for monoenergetic electrons of various energies. From Glendenin (Gl48).

(Gl48) shows some end points in aluminum for both beta emitters and homogeneous groups as a function of energy. There is little difference between the two if we plot maximum spectrum energies for the beta emitters.

7.7· Ionization loss—theory

Ionization loss theory for electrons, as distinguished from the theory for other charged particles, must consider the fact that after the "projectile" (electron) has struck a "target" (electron) we cannot tell which was initially which. A billiard ball can transfer *all* its kinetic energy in a head-on collision with a similar, resting ball. In the electron case, however, we logically will choose to identify the "projectile" electron as that particle which has the greater energy after the collision. A projectile electron so defined can give up at most only *one-half* of its kinetic energy in a head-on collision. If it gave up more, we would cease to label it as the projectile. In addition, there are quantum-mechanical exchange effects that must be considered when the projectile and the target are identical particles. Neither of these considerations apply to positrons. We give here two limiting cases of the general theoretical expression for the collision loss of negatrons of kinetic

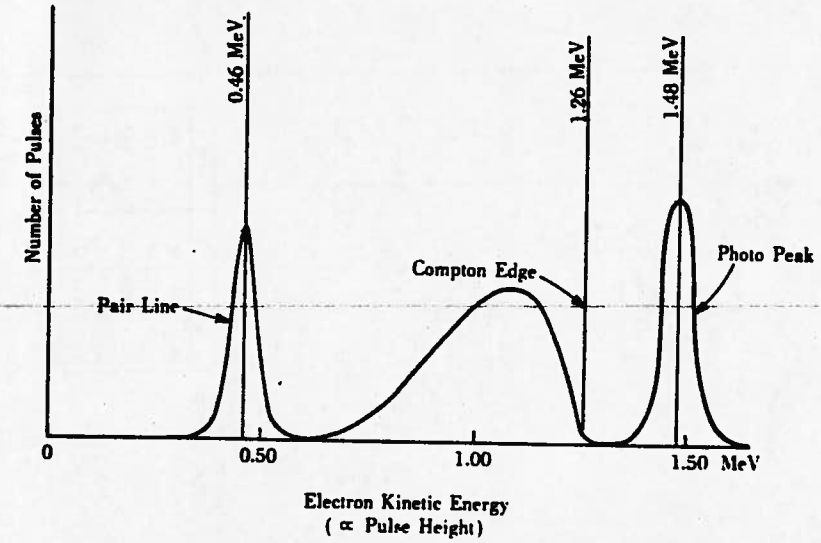

Figure 8-4 Idealized pulse-height spectrum for a scintillator detecting 1.48 MeV photons.

The Compton effect provides a simple method of determining the energy of a photon. From Equation 4-11 we have

$$E_k = E - E_0 = h\nu - h\nu'$$

Because $\nu = c/\lambda$ and $\nu' = c/\lambda' = c/(\lambda + \Delta\lambda)$, we may write this as

$$E_k = h\nu \frac{\Delta\lambda}{\lambda + \Delta\lambda} \qquad [4\text{-}16]$$

where $\Delta\lambda$ depends on the scattering angle θ and is given by Equation 4-15. The kinetic energy of the recoil electron is a maximum, $E_{k,max}$, when a head-on collision occurs, the electron recoiling in the forward direction and the scattered photon traveling in the backward direction. In such a collision $\theta = 180°$ and $\Delta\lambda = 2h/m_0c$, and Equation 4-16 becomes

$$E_{k,max} = h\nu\left(\frac{(2h\nu/m_0c^2)}{1 + (2h\nu/m_0c^2)}\right) \qquad [4\text{-}17]$$

Consider the pulse-height distribution, or spectrum, shown in Figure 8-4. The number of detected pulses for a given pulse height is displayed as a function of the pulse height, which is measured in volts but shown here as kinetic energy of the electrons in MeV. The monochromatic gamma-ray source in this case consists of radioactive ^{40}K atoms, each one of which emits a photon of 1.48 MeV as the unstable nucleus decays.

The peak of highest energy originates from the photoelectric effect. Since the binding energy of atomic electrons is only a few electron volts, small compared with the photons' energy, and consequently the photoelectrons have essentially the entire photon energy, the energy at the so-called "photopeak" is almost exactly the same as the gamma-ray energy. The second peak arises from the Compton effect. When a 1.48 MeV photon collides head on with an essentially free atomic electron, the Compton electron recoils in the forward direction with a kinetic energy of 1.26 MeV (computed from Equation 4-17), while the scattered photon travels in the reverse direction with the remaining energy, 1.48 − 1.26, or 0.22, MeV. Compton collisions that are not head-on produce less energetic electrons and more energetic scattered photons. Therefore, the Compton peak has a relatively sharply defined high-energy edge, in the figure corresponding to 1.26 MeV; it trails off gradually on the low-energy side because of the Compton collisions producing electrons with less than the maximum kinetic energy. The third peak in the scintillation spectrum originates from electron-positron pair production. Since the rest energy of an electron or positron is 0.51 MeV, a total of 1.02 MeV is needed to bring a pair into existence. The difference in energy, 1.48 − 1.02 = 0.46 MeV, is the sum of the kinetic energies of the electron and positron (see Section 4-5); this total kinetic energy, after exciting scintillator electrons, produces the pulses at the pair-production peak.

The relative sizes of the three peaks described depend on the energy of the photons and the size, shape, and identity of the scintillation material. Still other peaks may be found. For example, gamma rays with an energy above the threshold energy of 1.02 MeV for pair production will produce positrons, and if the positrons are annihilated with electrons before leaving the scintillator, annihilation photons of 0.51 MeV are produced (Section 4-5), and these photons also can give rise to photoelectric and Compton peaks.

From - Elementary Modern Physics 2nd Ed by Weidner and Sells

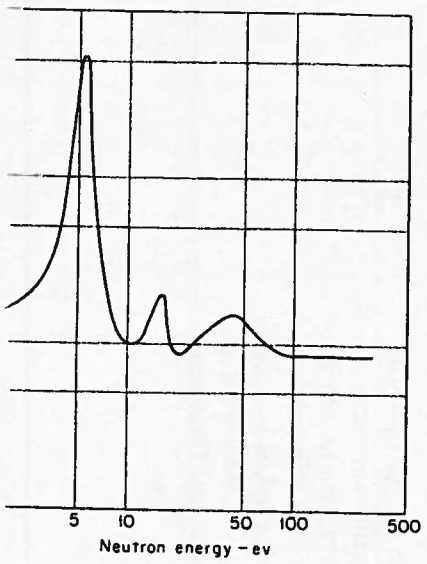

FIG. 20.9 Nuclear cross-section of silver. [Rainwater, Havens, Wu, and Dunning, *Phys. Rev.* 71, 65 (1947)].

.EAR DECAY SCHEMES

ission of a γ-ray a nucleus falls from an excited state to some lower state. The γ-ray emission of the nucleus is analogous to the emission en an atom falls from an excited state to a lower state. In both cases, E_1. When a nucleus emits a β particle, the daughter nucleus is an excited state and can reach a more stable state by emission of a on. Examples of decay schemes are shown in Fig. 20.10.

r, for instance, the decay of ^{60}Co in (d). In almost every case it 12 mev β^- to yield ^{60}Ni in an excited state. This ^{60}Ni passes almost ously to the ground state by emission of two successive α-ray photons. in 10^4 times, however, the ^{60}Co emits a 1.478 mev β^-.

STRUCTURE OF THE NUCLEUS

ent of mechanics knows that it is not possible to obtain an analytic the *three-body problem*, i.e., the motions of three masses under the their mutual gravitational interactions. As the number of inter- es increases, so does the mathematical difficulty, so that many-body ust be attacked by approximation methods. Also, in the nuclear w of force between the nucleons is not well understood. Thus we do ny exact theory of the structure of a nucleus composed of Z protons rons interacting together with attractive exchange forces as well as repulsions between the protons. The best we can do is to work

For Exp # 15
From Physical Chemistry by W.J. Moore

with simplified models. Two such models have been used with success, the *shell model* and the *collective model*.

The shell model was suggested by analogy with the shell model of the electronic structure of atoms. The very stable *magic-number nuclei* were reminiscent of the closed electron shells of the inert gases. The nuclear model is more complicated since there is no central field of force, and two kinds of nucleon must be accommodated.

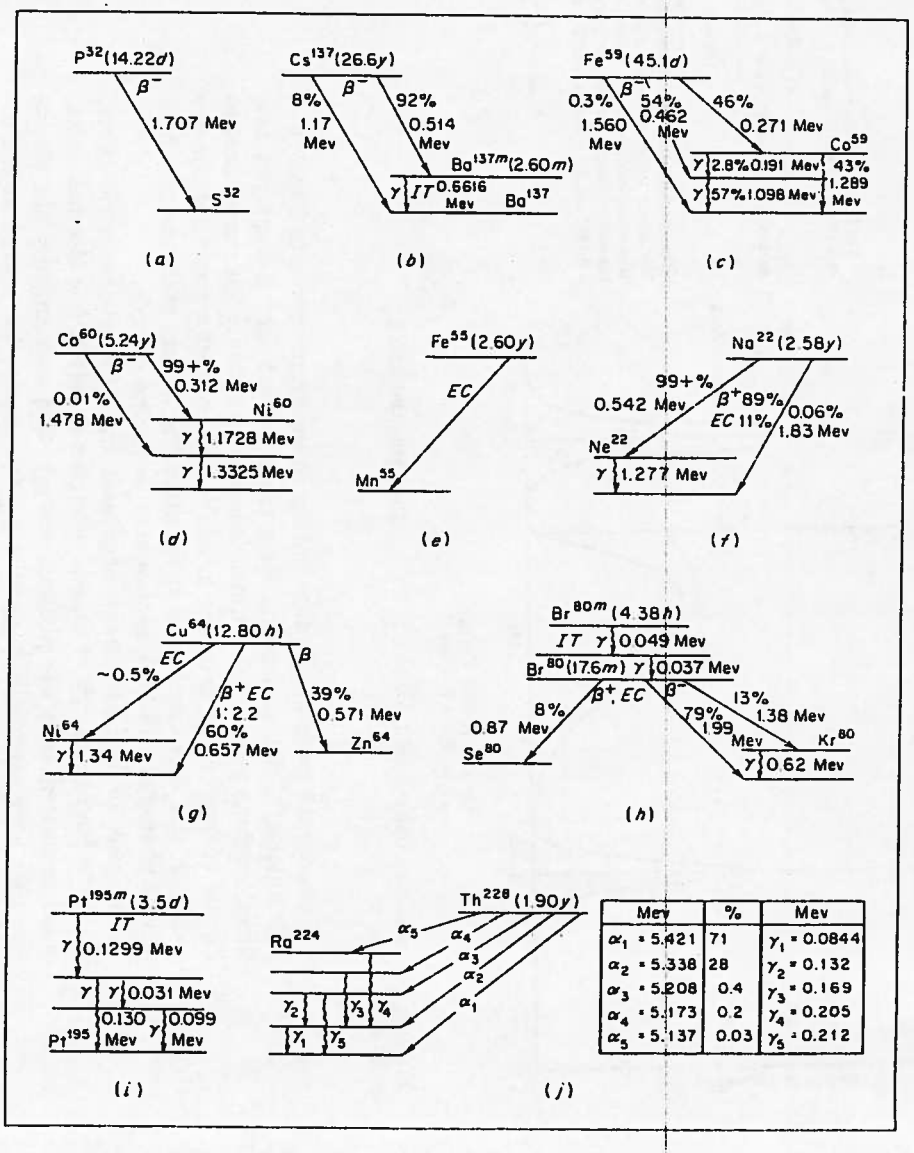

FIG. 20.10 Examples of decay schemes of radioactive nuclides. [R. T. Overman

At high enough speeds, the second and third terms in the square brackets become important. The curve passes through a broad minimum and increases slowly thereafter as v increases. Figure 6 shows plots of $(-dE/dx)_r$ in standard air for various particles. The curve rises at high energies because, according to the theory of relativity, the electric field set up by a moving charge tends to concentrate itself in the plane normal to the motion as the speed increases. This means that the electric-field

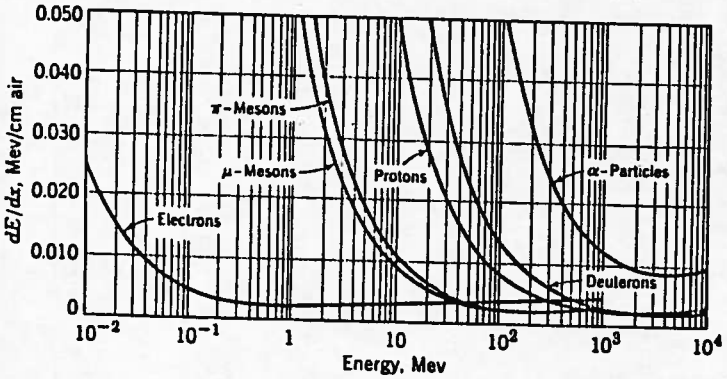

FIG. 6. The stopping power of standard air for different particles at different energies.

strength can exert an effect farther from the particle track and thus produce more ions than it otherwise could. The relativistic effect was already taken into account by Bohr in his 1915 classical treatment of the energy-loss problem (B15).

In combining Eq. 7 with Eq. 8 to calculate mean ranges, we must remember that Eq. 8 fails at low energy. We get around this by writing

$$\bar{R} = \bar{R}' + \int_{E'}^{E_0} (-dE/dx)^{-1}\, dE \tag{9}$$

where $\bar{R}'$, E' represent a point known empirically on the range-energy curve (5 Mev $< E' < E_0$).

By means of Eq. 7 we can find a range-energy curve for one ionizing particle, given the curve for another. Combining Eqs. 7 and 8 leads to

$$\bar{R} = z^{-2}\int_0^E f(v)\, dE = mz^{-2}F(v) \tag{10}$$

where m is the mass of the particle (not of the electron). This says that for different particles in a given absorber the range depends only upon the particle speed, its mass, and its charge. $F(v)$ and $f(v)$ are functions whose values may be worked out if desired; they do not contain z or m.

If we compare two particles of masses m and m_0 and charges z and z_0 and identical speeds, their ranges in the same absorber will be given, according to Eq. 10, by

$$\bar{R} = \bar{R}_0(m/m_0)(z_0/z)^2 \tag{11}$$

Their energies must be related by

$$E = E_0(m/m_0) \tag{12}$$

if the speeds are to be the same. Let m_0 and z_0 describe the alpha particle, and m and z the proton; we can then start with the alpha range-energy curve and, pointwise, plot out that for protons. The point (7.00 Mev, 5.92 cm) is on the alpha curve, for example. From Eq. 12 a proton of $E = 7.00\ (1.01/4.00)$ Mev $= 1.77$ Mev has the same speed. From Eq. 11 the range of such a proton is $5.92\ (1.01/4.00)(2/1)^2$ cm $= 5.98$ cm. Thus $E = 1.77$ Mev and $\bar{R} = 5.98$ cm is the corresponding point on the proton curve.

These considerations hold strictly only for $z = z_0$. In such cases (H^1, H^2, H^3 and all positive mesons, for example) the capture and loss of electrons is the same for both particles. Because of this, Eq. 11 is rather exact even though capture and loss was not considered in deriving Eq. 8. Range-energy curves for mesons in photographic emulsion can thus be computed if the curve for protons in emulsion is known (B50). For the proton-alpha particle relationship, the fact that the capture and loss is different for the two particles means, empirically, that we must substitute

$$\bar{R} = \bar{R}_0 M z_0^2/M_0 z^2 - 0.20 \text{ cm} \tag{13}$$

for Eq. 11. This gives $\bar{R} = 5.78$ cm in our example instead of 5.98 cm. This correction will be relatively less important at higher energies.

ELECTRONS

7.6· Absorption—low energies

At "low" energies the energy loss of electrons in matter is due to ionization and excitation processes. Figure 7 shows a typical semilogarithmic absorption plot for the negatrons from P^{32}; they form a continuous group whose maximum energy is 1.71 Mev. There is an *end point* R, beyond which there are no particles ($\sim$810 mg/cm^2).

Beta-ray end points are not as well defined as alpha-ray ranges (compare Figs. 7 and 4). This is because (1) nuclear electrons have a continuous distribution in initial energy, whereas the alpha